Conference paper

Ana C. Mendes*, Elhamalsadat Shekarforoush, Christoph Engwer, Sophie R. Beeren, Christian Gorzelanny, Francisco M. Goycoolea and Ioannis S. Chronakis

Co-assembly of chitosan and phospholipids into hybrid hydrogels

Abstract: Novel hybrid hydrogels were formed by adding chitosan (Ch) to phospholipids (P) self-assembled particles in lactic acid. The effect of the phospholipid concentration on the hydrogel properties was investigated and was observed to affect the rate of hydrogel formation and viscoelastic properties. A lower concentration of phospholipids (0.5 % wt/v) in the mixture, facilitates faster network formation as observed by Dynamic Light Scattering, with lower elastic modulus than the hydrogels formed with higher phospholipid content. The nano-porous structure of Ch/P hydrogels, with a diameter of 260 ± 20 nm, as observed by cryo-scanning electron microscopy, facilitated the penetration of water and swelling. Cell studies revealed suitable biocompatibility of the Ch/P hydrogels that can be used within life sciences applications.

Keywords: biomaterials; carbohydrates; chitosan; colloids; EUCHIS-12; hydrogel; ICCC-13; phospholipids; self-assembly.

Introduction

Hydrogels are three-dimensional (3D) structures made of chemical or physical crosslinked polymeric networks with a high ability to absorb and retain large amounts of water [1–5]. Hydrogel properties such as soft and rubbery consistency and diffusive transport characteristics [6], gives them the possibility to be used as scaffolds for cell growth and proliferation [1]. In addition, some hydrogels have mucoadhesive and bioadhesive characteristics [2]. Moreover, hydrogels offer the advantage of flexibility to deform and conform to the shape they are confined to, which makes them good candidates to be used in a broad range of food [7] and biomedical applications [1–5].

Among other natural derived polymers, chitosan(s) (polysaccharides made of glucosamine and N-acetyl glucosamine units), exhibit a set of remarkable biological properties such as biocompatibility, biodegradability, hemostatic activity, antibacterial, antimycotic and anticoagulant activity [8–11]. Furthermore, the degradation products of chitosan have been shown to be nontoxic, non-immunogenic and noncarcinogenic [12]. Consequently chitosan(s) have been widely formulated into several structures such as fibers, films,

*Corresponding author: Ana C. Mendes, Nano-BioScience Research Group, DTU-Food, Technical University of Denmark, Søltofts plads 227, 2800 Kgs. Lyngby, Denmark, e-mail: anac@food.dtu.dk
Elhamalsadat Shekarforoush and Ioannis S. Chronakis: Nano-BioScience Research Group, DTU-Food, Technical University of Denmark, Søltofts plads 227, 2800 Kgs. Lyngby, Denmark
Christoph Engwer and Francisco M. Goycoolea: Institute for Biology and Biotechnology of Plants (IBBP), Westfälische Wilhelms-Universität Münster, Schlossgarten 3, 48149 Münster, Germany
Sophie R. Beeren: DTU-Chemistry, Technical University of Denmark, Kemitorvet 207, 2800 Kgs. Lyngby, Denmark
Christian Gorzelanny: Experimental Dermatology, Medical Faculty Mannheim, Heidelberg University, Theodor-Kutzer-Ufer 1-3, 68167 Mannheim, Germany

particles and hydrogels and used in a wide range of biomedical applications such as drug delivery and tissue engineering [1, 13, 14]. Chitosan(s) physical hydrogels can be produced via non-covalent interactions e.g. electrostatic, hydrophobic, and hydrogen bonding forces between polymer chains [1]. The properties of physical hydrogels can be easily tuned by adjusting the concentration and nature of the components. Furthermore these hydrogels are prepared often in mild conditions (as they don't require toxic covalent crosslinkers), making their use safe for medical applications. Examples of chitosan physical hydrogels are numerous and have been well described elsewhere [1, 15].

Phospholipids, the self-assembling molecular building blocks of cell membranes, constituted by a charged polar head group and a hydrophobic tail, have been largely explored to produce nano-bio structures in the shape of nanoparticles, capsules/liposomes, emulsions [12] and organogels [16]. Organogels, the 3-D networks of entangled reverse cylindrical micelles and jelly- like phases, immobilizing macroscopic external organic phases [17], have been developed by using lecithins as building blocks [16].

The binding of chitosan to phospholipids is a phenomenon known to be caused by the destabilization of the phospholipid membrane bilayer when exposed to chitosans [18, 19] as a consequence of the binding of the negatively charged phosphate groups in phospholipids to chitosan(s) [20]. Formulation of hybrid stable films of chitosan-phospholipids for the release of paclitaxel [21] and docetaxel [22, 23], assembled nanoparticles [24, 25] and nanocapsules/nanoparticles to release capsaicin [26], have been reported. In addition, the biocompatibility of chitosans/phospholipids systems [12, 27] has been confirmed, highlighting the benefits of using these components to produce nanostructures to be used within life sciences. Recently our group explored the potential of combining chitosan with phospholipids to produce electrospun chitosan/phospholipids hybrids nanofibers for applications in drug delivery [28], demonstrating the potential of combining both components to develop functional chitosan/phospholipids hybrids. However, to the best of our knowledge, the co-assembly of chitosan and phospholipids to fabricate hydrogels has never been studied. Therefore, this study aimed to develop hybrid chitosan/phospholipids hydrogels and investigate their physicochemical properties and biocompatibility.

Materials and methods

Materials

Chitosan, with Molecular weight (Mw) of 385 kDa, Degree of Acetilation (DA) of 26 % was obtained from GILLET CHITOSAN (product 111). Asolectin from soybean (containing approximately 25–33 % of lecithin, cephalin and phosphatidylinositol, 24 % saturated fatty acids, 14 % mono-unsaturated and 62 % poly-unsaturated fatty acids) and chemicals were obtained from Sigma-Aldrich, unless otherwise indicated. All of the consumable were used as received.

Fabrication of hybrid chitosan/phospholipids hydrogels

Asolectin was suspended in lactic acid (2 M) at concentrations of 0.5, 1 and 2 % wt/v. Solutions of asolectin were centrifuged to remove undissolved components. Chitosan was added to asolectin solutions in order to reach a concentration of 2 % wt/v. Samples were mixed until hydrogel formation took place (for about 4 min) and named as Ch/P0.5, Ch/P1 and Ch/P2, for phospholipids concentrations of 0.5, 1 and 2 % wt/v, respectively.

[1]H nuclear magnetic resonance (NMR) spectroscopy

^{1}H NMR spectra were recorded on an 800 MHz Bruker (Fällanden, Switzerland) Avance spectrometer equipped with a TCI Z-gradient CryoProbe and an 18.7 T magnet (Oxford Magnet Technology, Oxford, UK) and processed

with Topspin 3.0 (Bruker). The samples were prepared in the same manner as described for hydrogel preparation in D_2O. To facilitate the transfer of the hydrogel to the NMR tubes, the samples were warmed with a heat gun.

Dynamic light scatering (DLS) measurements

ζ-Potential and size measurements were performed using a Zetasizer NanoZS Instrument (ZEN 3600, Malvern Instruments, Worcestershire, UK). Prior the analyzes, phospholipids and chitosan/phospholipid solutions were prepared with the same concentrations used in the hydrogels. The solutions were filtered using a pyrogen free 0.45 mm disposable membrane filter (Schleicher and Schuell Bioscience, Germany). The intensity correlation function (ICF) was recorded at a fixed laser position (3 mm) and laser intensity (attenuator 7) was optimized prior to the measurements. The ICF was recorded over 100 seconds at 25 °C. The experiments were performed in three replicates. For data analysis, the ICF was normalized.

Rheological analysis

The viscoelastic properties (elastic (G') and viscous modulus (G'')) of hydrogel samples were examined by low amplitude oscillatory measurements using a Thermo Scientific™ Haake Mars II Rheometer System. A serrated PP 60Ti (plate–plate geometry) with a gap of 1 mm, at 25 °C was utilized. The sample was loaded on the rheometer plate and frequency sweep using a constant shear stress of 1 Pa (within the linear viscoelastic region) and stress sweep (at a frequency of 1 Hz) were carried out. The samples were covered with silicone oil to avoid evaporation. All experiments were prepared in triplicate for each sample.

Hydrogel morphology

The morphology of the hydrogels was evaluated by cryo-scanning electron microscopy (cryo-SEM). The cross-sections of the hydrogel were analyzed, applying a cryogenic technique to fracture the samples, before sputter-coating with gold prior the visualization on a scanning electron microscope with cryo-function coupled (Quanta FEG 3D SEM).

Water uptake

The amount of water uptake (swelling) was determined by immersion of the samples in PBS and incubation at 37 °C over a period of 1, 3, 6, 24 and 72 h in dynamic conditions. After each time point, samples were taken out of the solution, rinsed with distilled water, blotted on filter paper to remove surface water, and immediately weighed (mt, mass of wet sample). Afterwards, samples were dried until constant weight (mf) and the percentage of water uptake was determined following equation 1:

$$\text{WU } (\%) = \left(\frac{mt - mf}{mf} \right) \times 100 \tag{1}$$

Three replicates were performed for each sample [N = 3].

Weight loss

The stability of these hydrogels was evaluated thought the determinations of weight loss (WL). Samples were weighted, immersed in PBS and incubated at 37 °C under dynamic conditions during 1, 3, 6, 24 and 72 h. After

each time point, samples were taken out of the solution, rinsed with distilled water, blotted on filter paper (to remove surface water) and then dried until constant weight in order to determine the percentages of weight loss following equation:

$$WL\ (\%) = \left(\frac{mf - m0}{m0} \right) \times 100 \qquad (2)$$

where *mf* is the final mass after immersion and *m0* is the initial mass prior the immersion in PBS. Three replicates were performed for each sample [N = 3].

Biological assessment. LDH assay

The assay was performed as previously reported [29]. Briefly, hydrogels were placed with a spatula to the center of a well of a 12-well plate. The covered area was in the range of 0.7 cm^2 corresponding to 20 % of the total growth area. Prior to the LDH analysis 0.15 × 10^6 mouse fibroblasts (L929) were seeded into each well and cultivated for 24 h and 48 h. L929 cells were maintained in RPMI 1640 medium supplemented with 10 % fetal calf serum (FCS), 1 % L-glutamine and 1 % penicillin/streptomycin. LDH was measured in the supernatants of cells using a cytotoxicity test kit (Roche Diagnostics, Mannheim, Germany) according to the manufacture's protocol. Fluorescence microscopy and cell cycle analysis. L929 cells were fixed with ice-cold methanol for 30 min, washed with HEPES-buffered Ringer solution (140 mM NaCl, 5 mM KCl, 1 mM MgCl$_2$; 1 mM CaCl$_2$, 5 mM glucose and 10 mM HEPES) and blocked for 1 h at room temperature with 2 % bovine serum albumin (BSA) dissolved in HEPES-buffered Ringer solution, supplemented with 0.3 % Triton X-100. F-actin was stained for 1 h with TRITC-palloidin (Sigma-Aldrich, St. Louis, US) applying a 1:2000 dilution in HEPES-buffered Ringer solution. Nuclei were stained for 10 min with 4,6-diamidino-2-phenylindole (DAPI) diluted in HEPES-buffered Ringer solution (0.1 μg mL^{-1}). Fluorescence microscopy was employed using a Zeiss Z.1 observer (Zeiss, Jena, Germany) using a 20× objective. As basis for the cell cycle analysis DNA concentration per cell was analyzed using image J [30].

Results and discussion

NMR spectroscopy

The ^{1}H-NMR spectrum of asolectin in lactic acid (2 M) was recorded at three different concentrations: 0.5, 1 and 2 % wt/v (Fig. 1). Aside from the dilution factor, the spectra were essentially identical and each
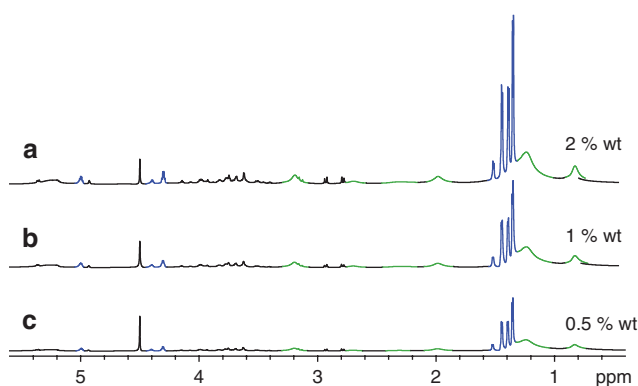

Fig. 1: ^{1}H-NMR spectra (800 MHz, 323 K) of asolectin/ lactic acid (2 M) in D$_2$O at varying concentrations: (a) 2 % wt/v; (b) 1 % wt/v and (c) 0.5 % wt/v.

showed broad signals for the hydrophobic tails of the phospholipids. When the phospholipids were present as monomers in solution, sharp signals with clear splitting patterns corresponding to each of the protons on the hydrocarbon tails of the phospholipids could be expected. The broad peaks suggest that instead the phospholipids have self-assembled into supramolecular particles. That the spectra are essentially identical indicates that the concentration of 0.5 % wt/v of asolectin in lactic acid solution is above the critical aggregation concentration and that the particles have similar structures within the concentration range studied.

The hydrogel and its individual constituent components were each analyzed using ¹H-NMR spectroscopy (Fig. 2). Figure 2a shows the ¹H NMR spectrum of the 2 M lactic acid solution used to prepare the hydrogel. Both free D,L-lactic acid and D,L-lactic acid oligomers, which form reversibly in aqueous solution via an ester condensation reaction, were identified [31]. Figure 2b shows the spectrum of chitosan (0.5 % wt/v) in the lactic acid solution. The signals for chitosan are identifiable, but broad, most likely because this large polymer has reduced mobility in the solution, which leads to line broadening [32]. In the presence of chitosan, several signals from the lactic acid broaden and shift upfield. This is most likely a consequence of the proton transfer from the carboxylic acid of lactic acid to the amines on the chitosan polymer and a consequent, electrostatic interaction between the positively charged polymer and the negatively charged lactate counterions. The signals that shift and broaden correspond to protons adjacent to the carboxylate groups. Figure 2c shows the spectrum of a solution of asolectin (2 % wt/v) and lactic acid (2 M). As asolectin is a mixture of different phospholipids, the ¹H-NMR spectrum is complex and no attempt was made to assign all the signals. It is possible, however, to identify the broadened signals due to the aliphatic protons in the hydrophobic tails of the phospholipids (colored green). These so broad signals are an indication that the phospholipids self-assemble in aqueous solution, presumably due to the hydrophobic effect.
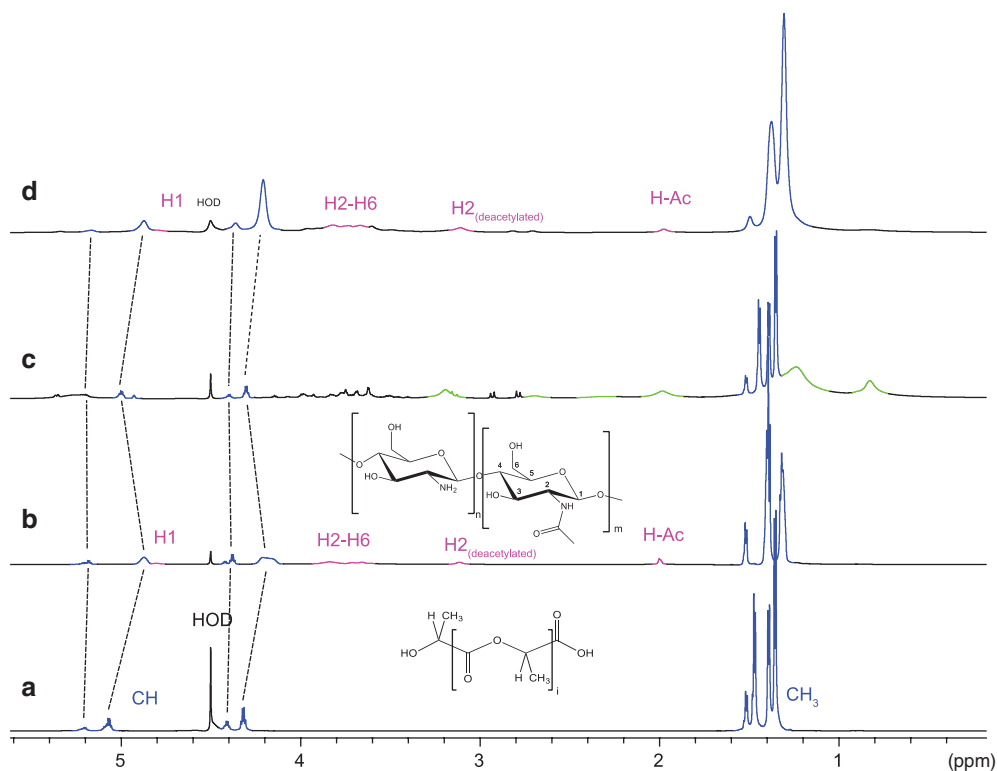

Fig. 2: ¹H-NMR spectra of (800 MHz, 323 K) of the hydrogel and its individual components in D₂O: (a) 2 M lactic acid; (b) chitosan (0.5 % wt/v) in 1 M lactic acid (the spectrum is amplified 2 times); (c) asolectin (2 % wt/v in 2 M lactic acid; and (d) the hydrogel formed with 2 % wt/v chitosan, 2 % wt asolectin and 2 M lactic acid.

In the NMR spectrum of the hydrogel (Fig. 2d) it is possible to clearly identify broad signals due to the chitosan and lactic acid components. However, the signals due to the hydrophobic tails of the asolectin component are conspicuously absent. Signals for gelators frequently become invisible in ^{1}H-NMR spectroscopy upon hydrogel formation due to extensive line broadening [33]. Notably the chitosan and lactic acid signals are still visible which suggests these components, on the other hand, have sufficient thermal motion in the hydrogel to provide the ^{1}H NMR spectrum. The residual water signal at 4.5 ppm is also broadened in the spectrum of the hydrogel, which indicates that the water molecules are also part of the gel assembly, as expected.

DLS

DLS analysis suggests the presence of self-assembled asolectin particles in solutions of lactic acid (2 M), as observed using NMR spectroscopy (Fig. 1). Increasing the concentration of phospholipid leads to a decrease of ζ-potential (Fig. 3a) and an increase in average diameter (Fig. 3b). The ζ-potential is related to the stability of charged particles in suspension [34]. The greater value of the ζ-potential (−48.2±1.5 mV) obtained at
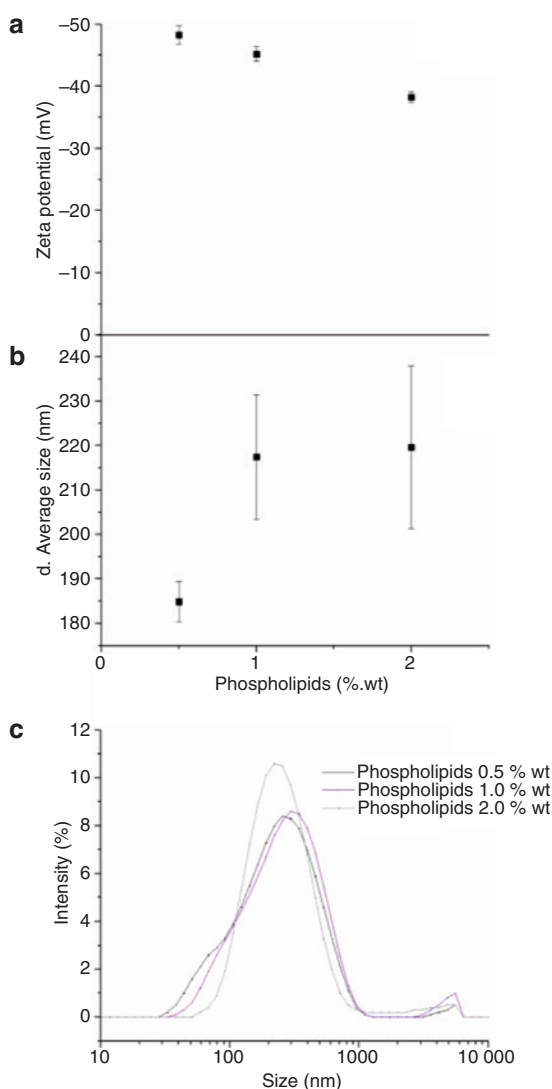

Fig. 3: The effect of the concentration of phospholipids on (a) zeta-potential, (b) d-particle size and (c) particle size distribution of self-assembled phospholipid nanoparticles at concentrations of 0.5, 1 and 2 % wt/v.

lower concentrations of phospholipids (Fig. 3a) might be related with the higher mobility of the phospholipid chains and thus favorable intermolecular interactions between them, leading to the formation of particles with a small average diameter of 185 ± 4.5 nm (Fig. 3b). Small and co-workers observed by DLS studies that the size of the lipid particles is proportional to the phospholipid concentration [35]. Furthermore, Chuah and co-workers [25] observed a similar trend: for higher concentrations of phospholipid molecules, the formation of larger and less stable particles was observed. At the highest concentration of phospholipid (2 % wt/v) the ζ-potential was found to be of -38.9 ± 0.3 mV (Fig. 3a) and the particle size was found to be 220 ± 18 nm (Fig. 3b). DLS analysis shows a narrow size distribution, suggesting that the concentration of phospholipid doesn't affect significantly its dispersity in solution (Fig. 3c).

DLS was also used to analyze the dynamic processes occurring in dispersions using the intensity correlation function (ICF), $g^{(2)} - 1$ [36]. Figure 4a shows a similar decay of ICF for all the tested phospholipid solutions in lactic acid, corresponding to the population of vesicles in solution. However after the addition of chitosan to each phospholipid solution, the initial intensity of ICF (s) decreased and a noisy/oscillatory signal appeared for longer delay times (Fig. 4). The decrease of ICF initial intensity has been correlated with the crosslinking of polymeric chains during hydrogel formation [36]. The fluctuations observed after the decay of ICF are related to the onset time of gelation [36, 37]. The data presented in Fig. 4 clearly demonstrate that the amount of phospholipid affects hydrogel formation. The initial decrease of ICF intensity (from phospholipid solution to hydrogel) was found to be more accentuated for Ch/P0.5 hybrid hydrogel (Fig. 4b). For this ratio
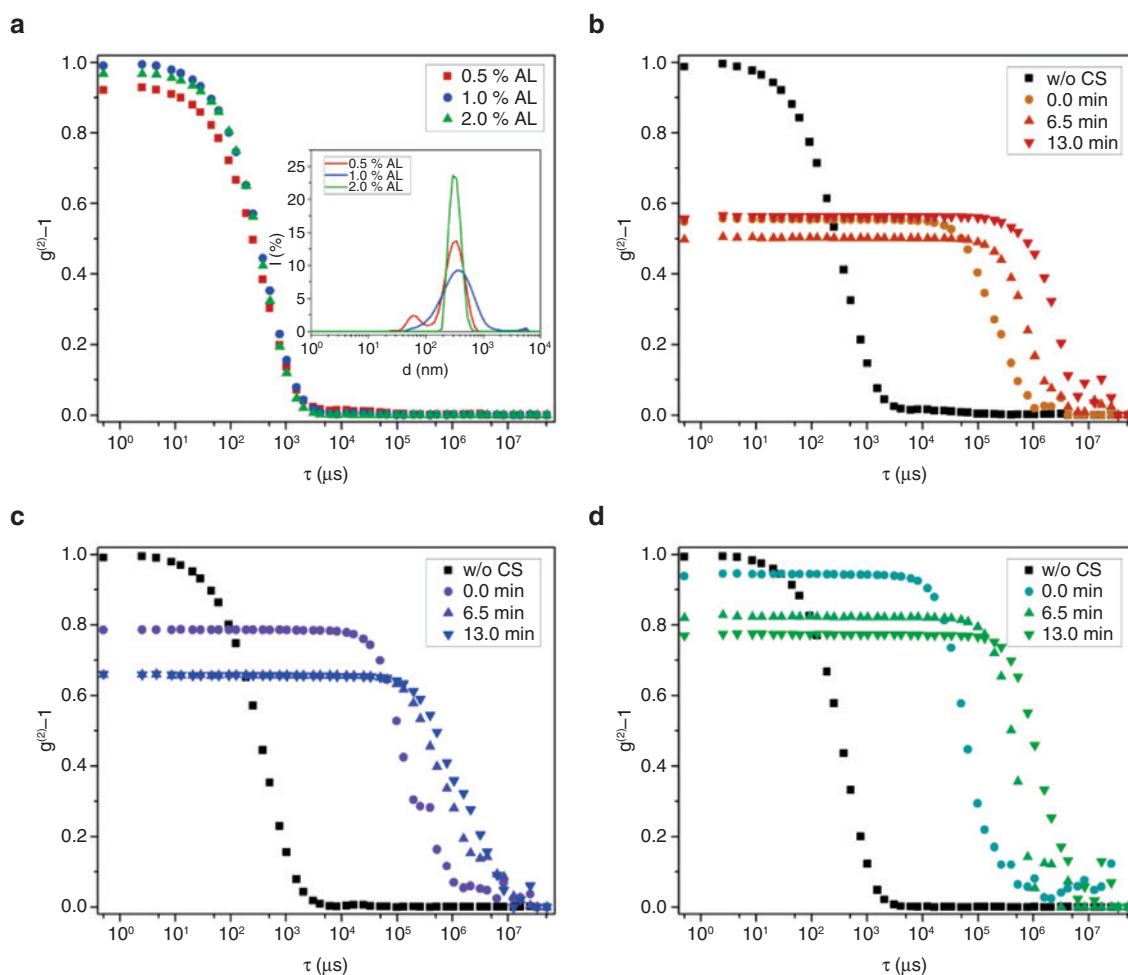

Fig. 4: Development of the intensity correlation function over time of different concentrations of (a) phospholipids; after the addition of chitosan and hydrogel formation using (b) 0.5 % wt/v, (c) 1 % wt/v and (d) 2 % wt/v of phospholipids.

the ICF intensity dropped from 0.99 to 0.56, while for Ch/P1 and Ch/P2 a decrease in the initial ICF intensity was observed from 0.99 to 0.79 and 0.93, respectively. This data suggests that the rate of gelation tend to decrease with increasing phospholipid content, as a result of increased viscosity and decreased mobility of the molecules in solution. The decrease of $g^{(2)} - 1$, when T tends to infinite (∞) was observed as result of a decrease of ergodicity and hydrogelation [38, 39].

Rheology

The viscoelastic properties of the Ch/P hybrid hydrogels were studied by oscillatory rheology as a function of frequency and shear stress (Fig. 5a and b). Within the frequency range tested, the solid-like response (G'), is dominant over the viscous-flow (G''), with high frequency dependence mostly for elastic modulus. Moreover, the tan δ value (tan $\delta = G''/G'$) provides a convenient index of the proportion of elastic-like character. The tan δ value at the frequency of ~1 Hz is 0.277, 0.371 and 0.436 for Ch/P2, Ch/P1 and CH/P0.5 hydrogels, respectively. For other biopolymer hydrocolloid hydrogels such as gelatin, agarose, and carrageenan tan δ value was found to range from about 0.02 to 0.07 [40].

The elastic and loss modulus followed the power law relation G' or G'' (ω) $= K \omega^A$ at the frequency range of 0.1 – 30 Hz and it can be used to describe the behavior of the G' and G'' in a comparable manner (Table 1). For hydrogels, the plots of log G' and log G'' vs. log ω have zero slope, whereas for weak elastic gels, the plots have positive slopes and the values of K' are higher than those of K'' with the frequency dependency, as found for the Ch/P hydrogels.

The response to increasing amplitude of oscillation is shown in Fig. 5b. The elastic and loss modulus remain independent of deformation at imposed strains up to ~100 Pa, with the samples effectively flowing beyond that. This dependence of shear moduli on oscillatory strain is characteristic of a weak elastic gel.
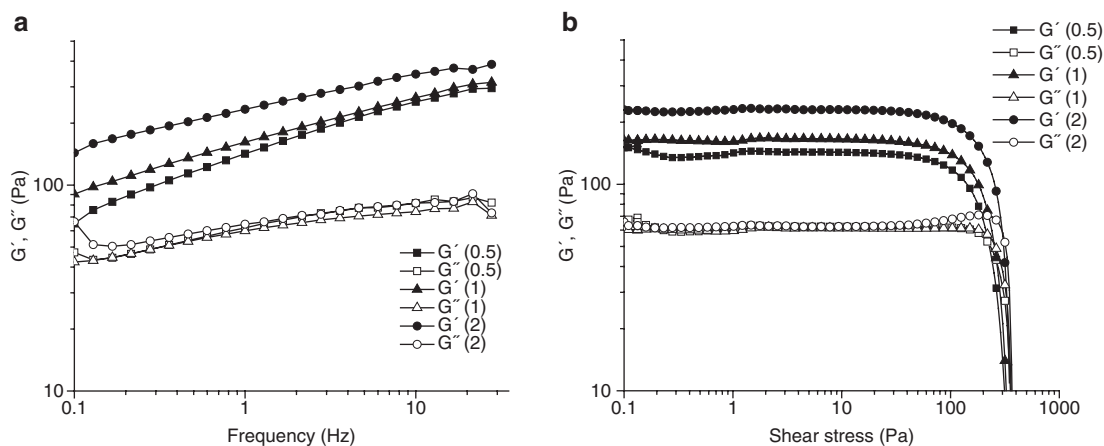

Fig. 5: Elastic (G') and viscous modulus (G'') of chitosan/phospholipids hybrid hydrogels as a function of frequency (a) and shear stress (b).

Table 1: Parameters from the power law relation $G(\omega) = K \omega^A$ determined from experimentally measured storage modulus and loss modulus for Ch/P hydrogels with different concentrations of phospholipids.

Sample designation	K'	A' (Pa s)	K''	A'' (Pa s)
Ch/P0.5	136.8	0.2669	60.0	0.1419
Ch/P1	158.5	0.2239	57.8	0.1216
Ch/P2	229.7	0.1717	63.5	0.1143

K' and A' refer to elastic modulus; K'' and A'' refer to viscous modulus.

Cryo-scanning electron microscopy (Cryo-SEM)

Figure 6, shows the internal microstructure of Ch/P hybrid hydrogels composed of a hierarchical porous structures, with porous diameter of 260 ± 20 nm. The different ratios of Ch/P provided similar morphology. Mertins and Dimova [20] have also observed that the adsorption of chitosan on the phospholipid membrane leads to the disruption of supramolecular phospholipids vesicles and pore formation. By phase contrast microscopy these authors observed the formation of microscopic pores during vesicle collapse and slower restructuring into microparticles resembling microgels [20].

Swelling

The swelling profile of the Ch/P hybrids over time is illustrated in the Fig. 7. Overall, it can be observed that the amount of phospholipid mediates the swelling capability of the Ch/P hybrid hydrogels. After 1 h, Ch/P0.5 absorbs about 0.62 that increased to 1.86 after 6 h in contact with PBS at 37 °C. Between 6 and 24 h the water uptake didn't change significantly and at the end of 72 h the swelling % was about 2.76. A Similar profile was observed for Ch/P1 and Ch/P2 hybrid hydrogels. The relatively rapid initial swelling (between 1 and 6 h) is mainly caused by the porous structure (Fig. 6) which facilitated the permeation of the PBS inside the hydrogels [41, 42]. The increase of phospholipid content tends to increase the swelling capability of these hydrogels due to the hydrophilic nature of asolectin. This feature might facilitate the diffusion of water through the inner porous existent within the hydrogel nano-micro structure and thus facilitate water absorption.
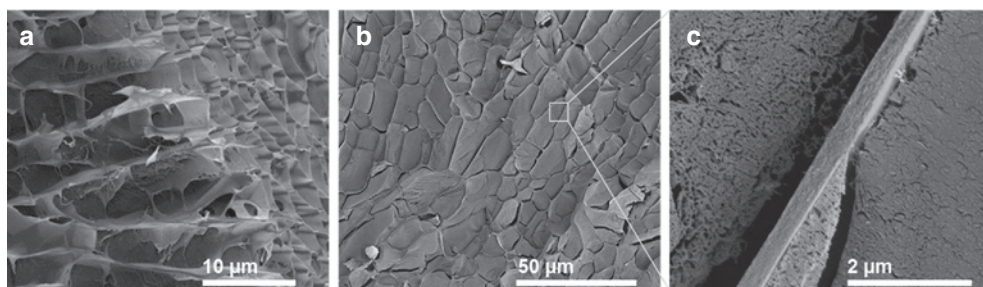

Fig. 6: Cyo-SEM images of the cross sections of Ch/P hybrid hydrogels, showing its internal porous micro (a) and nanostructures (b) and (c) at different magnifications.
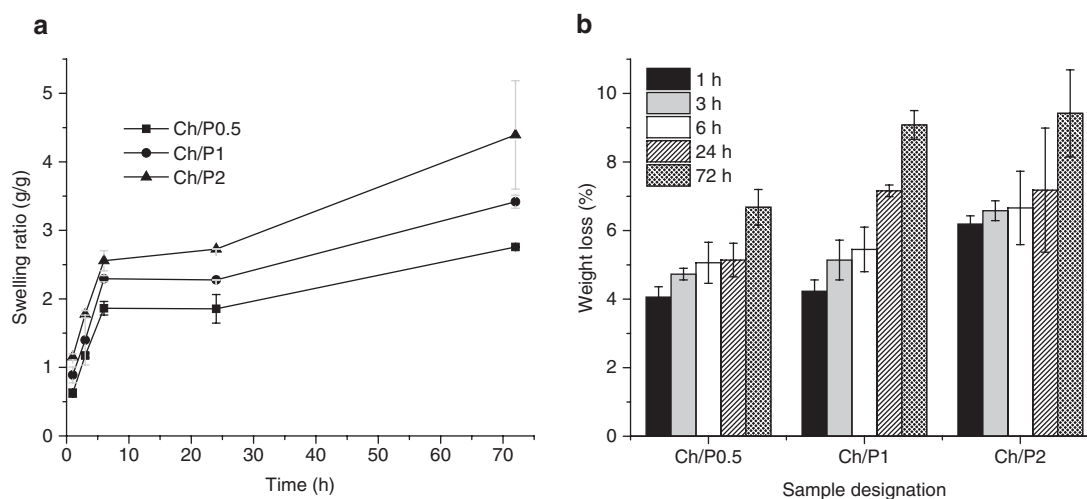

Fig. 7: The effect of the phospholipid content on the (a) swelling capability and (b) stability of the Ch/P hybrid hydrogels.

The stability of the Ch/P hybrid hydrogels was investigated by determination of their losses of weight. With the increase of the incubation time of the hydrogels in PBS, an increase in the percentage of the weight loss was observed. Thus, Ch/P0.5 lost about 4 % of its weight after 1 h of incubation within PBS and about 5 % after 24 h. At the end of the 72 h these hydrogels lost about 6.68 % of their weight. Comparable trends were
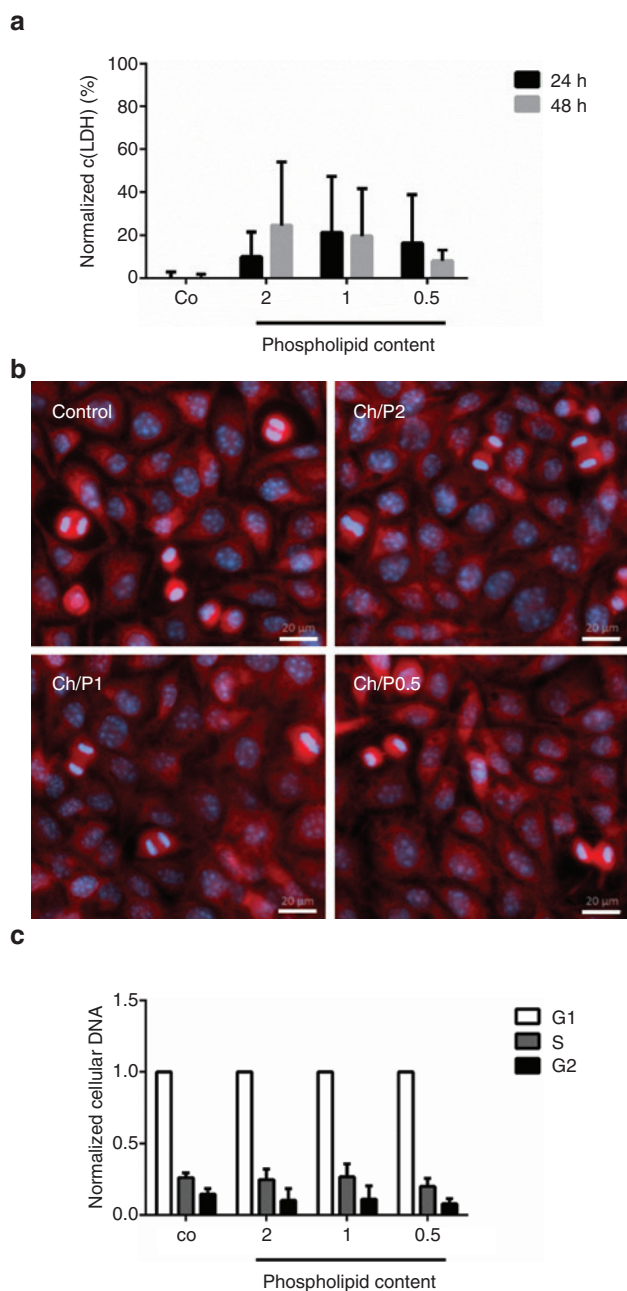

Fig. 8: Co-cultivation of chitosan/phospolipid hydrogels with fibroblasts (L929). (a) Concentration of lactate dehydrogenase (LDH) measured in the supernatants of cell cultivated for 24 h and 48 h in the presence or absence of hydrogels. Controls (co) were set to 0 %, cells treated with 0.1 % triton-X100 inducing a maximal release of LDH were set to 100 %. (N = 3); (b) Fluores-cence microscopic analysis of cells co-cultivate with hydrogels that were on glass cover slips. Cells seeded on glass cover slips without hydrogel were used as control (co). F-actin was stained with TRITC-labeled phalloidin (red), DNA of cell nuclei were stained with DAPI (blue). Scale bar corresponds to 20 μm; (c) DNA staining with DAPI was used to analyze the cell cycle status of L929 cells. (> 300 nuclei were analyzed of three independent experiments).

observed for the other hydrogel formulations (Ch/P1 and Ch/P2). Ch/P3 hydrogels lost about $1.4 \pm 0.1\%$ and Ch/P1 lost about $1.2 \pm 0.2\%$ more of their weigh compared to Ch/P0.5.

Biological assessment

Fibroblasts were co-cultivated with the phospholipid/chitosan hydrogels with different contents of phospholipids to investigate their biological compatibility. Potential cytotoxicity was accessed by measuring, the amount of lactate dehydrogenase (LDH) released into the supernatants 24 h and 48 h after seeding the cells. In comparison to the control cells (cultivation on tissue culture treated polystyrene), increased levels of LDH released were detected in the supernatants of the cells co-cultivated with hydrogels. However, differences between the groups were not statistically significant (Fig. 8a). To further supplement these findings, immunofluorescence staining of the cells was analyzed by fluorescence microscopy (Fig. 8b). In preliminary experiments it was found that cells barely attached directly to the hydrogels but settle around the hydrogels. Therefore our examination was focused on areas next to the hydrogels. In agreement with the LDH measurements, no evident differences in cell morphologies or mitosis rate were found. These results were further confirmed by a cell cycle analysis indicating no negative impact of the hydrogels on the proliferative potential of L929 cells (Fig. 8c).

Conclusions

Asolectin phospholipid in 2 M lactic acid produced supramolecular particles with ζ-potential and size depending on the phospholipid concentration. The addition of chitosan (Mw 385 KDa, DA 26 %) to phospholipid self-assembled particles in lactic acid formed stable hybrid hydrogels. The concentration of phospholipid particles affected the rate of the hydrogel formation and on their viscoelastic properties. The lower concentration of phospholipids (0.5 % wt/v) facilitates faster network formation, with lower elastic modulus than the gels formed with higher phospholipid content. The internal structure of Ch/P hybrid hydrogels was found to involve nanoporous sections which in turn facilitated the penetration of water and swelling. Cell studies revealed that the cells didn't attach to the hydrogels, however they could perform their metabolic activity suggesting that these hybrid chitosan/phospholipids hybrid hydrogels have suitable biocompatibility to be used in life scienses applications.

References

[1]   N. Bhattarai, J. Gunn, M. Zhang, *Adv. Drug Deliv. Rev.* **62,** 83 (2010).
[2]   N. A. Peppas, J. J. Sahlin, *Biomaterials* **17,** 1553 (1996).
[3]   N. A Peppas, P. Bures, W. Leobandung, H. Ichikawa, *Eur. J. Pharm. Biopharm.* **50,** 27 (2000).
[4]   J. M. Shapiro, M. L. Oyen, *J. Miner. Met. Mater. Soc.* **65,** 505 (2013).
[5]   D. Buenger, F. Topuz, J. Groll, *Prog. Polym. Sci.* **37,** 1678 (2012).
[6]   M. Hamidi, A. Azadi, P. Rafiei, W. Hennink, C. van Nostrum, *Adv. Drug Deliv. Rev.* **54,** 13 (2002).
[7]   H. M. Shewan, J. R. Stokes, *J. Food Eng.* **119,** 781 (2013).
[8]   V. Balan, L. Verestiuc, *Eur. Polym. J.* **53,** 171 (2014).
[9]   R. Jayakumar, D. Menon, K. Manzoor, S. V. Nair, H. Tamura, *Carbohydr. Polym.* **82,** 227 (2010).
[10] Y. Luo, Q. Wang, *Int. J. Biol. Macromol.* **64,** 353 (2014).
[11] B. Menchicchi, A. Hensel, F. M. Goycoolea, *Curr. Pharm. Des.* **21,** 4888 (2015).
[12] R. Souza, P. Zahedi, C. J. Allen, M. Piquette-Miller, *Biomaterials* **30,** 3818 (2009).
[13] A. Anitha, S. Sowmya, P. T. Sudheesh Kumar, S. Deepthi, K. P. Chennazhi, H. Ehrlich, M. Tsurkan, R. Jayakumar, *Prog. Polym. Sci.* **39,** 1 (2014).

[14] W. W. Thein-Han, W. F. Stevens, *Drug Dev. Ind. Pharm.* **30,** 397 (2004).

[15] M. Dash, F. Chiellini, R. M. Ottenbrite, E. Chiellini, *Prog. Polym. Sci.* **36,** 981 (2011).

[16] V. K. Singh, P. M. Pandeyb, T. Agarwalb, D. Kumara, I. Banerjeeb, A. Anisc, K. Palb, *J. Mech. Behav. Biomed. Mater.* **55,** 250 (2015).

[17] A. Bhatia, B. Singh, K. Raza, S. Wadhwa, O. P. Katare, *Int. J. Pharm.* **444,** 47 (2013).

[18] N. Fang, V. Chan, H. Q. Mao, K. W. Leong, *Biomacromolecules* **2,** 1161 (2001).

[19] O. Mertins, R. Dimova, *Langmuir* **29,** 14545 (2013).

[20] O. Mertins, R. Dimova,. *Langmuir* **29,** 14552 (2013).

[21] J. Grant, M. Blicker, M. Piquette-Miller, C. Allen, *J. Pharm. Sci.* **94,** 1512 (2005).

[22] P. Zahedi, R. Souza,, M. Piquette-Miller, C. Allen, *Int. J. Pharm.* **377,** 76 (2009).

[23] E. A. Ho, V. Vassileva, C. Allen, M. Piquette-Miller, *J. Control. Release* **104,** 181 (2005).

[24] F. Sonvico, A. Cagnani, A. Rossi, S. Motta, M. T. Di Bari, F. Cavatorta, M. J. Alonso, A. Deriu, P. Colombo, *Int. J. Pharm.* **324,** 67 (2006).

[25] A. M. Chuah, T. Kuroiwa, S. Ichikawa, I. Kobayashi, M. Nakajima, *J. Food Sci.* **74,** N1 (2009).

[26] F. M. Goycoolea, A. Valle-Gallego, R. Stefani, B. Menchicchi, L. David, C. Rochas, M. J. Santander-OrtegA, M. J. Alonso, *Colloid Polym. Sci.* **290,** 1423 (2012).

[27] P. Pereira, S. S. Pedrosa, A. Correia, C. F. Lima, M. P. Olmedo, Á. González-Fernández, M. Vilanova, F. M. Gama, *Toxicol. Vitr.* **29,** 638 (2015).

[28] A. C. Mendes, C. Gorzelanny, N. Halter, S. W. Schneider, I. S. Chronakis, *Int. J. Pharm.* **510,** 48 (2016).

[29] C. Gorzelanny, R. Kmeth, A. Obermeier, A. T. Bauer, N. Halter, K. Kümpel, M. F. Schneider, A. Wixforth, H. Gollwitzer, R. Burgkart, B. Stritzker, S. W. Schneider, *Sci. Rep.* **6,** 22849 (2016).

[30] C. A. Schneider, W. S. Rasband, K. W. Eliceiri, *Nat. Methods* **9,** 671 (2012).

[31] J. L. Espartero, I. Rashkov, S. M. Li, N. Manolova, M. Vert, *Macromolecules*, **9297,** 3535 (1996).

[32] M. Lavertu, Z. Xia, A. N. Serreqi, M. Berrada, A. Rodrigues, D. Wang, M. D. Buschmann, A. Gupta, *J. Pharm. Biomed. Anal.* **32,** 1149 (2003).

[33] Y. E. Shapiro, *Prog. Polym. Sci.* **36,** 1184 (2011).

[34] A. C. Mendes, K. H. Smith, E. Tejeda-Montes, E. Engel, R. L. Reis, H. S. Azevedo, A. Mata, *Adv. Funct. Mater.* **23,** 430 (2013).

[35] D. M. Small, *Molecular Association in Biological and Related Systems* **84,** 31 (American Chemical Society, 1968).

[36] W. A. de Morais, M. R. Pereira, J. L. C. Fonseca, *Carbohydr. Polym.* **87,** 2376 (2012).

[37] K. Yoshida, T. Yamaguchi, N. Osaka, H. Endo, M. Shibayama, *Chem. Phys.* **12,** 3260 (2010).

[38] P. N. Pusey, W. Van Megen, *Phys. A Stat. Mech. its Appl.* **157,** 705 (1989).

[39] T. Norisuye, M. Shibayama, R. Tamaki, Y. Chujo, *Macromolecules* **32,** 1528 (1999).

[40] I. S. Chronakis, L. Piculell, J. Borgström, *Carbohydr. Polym.* **31,** 215 (1996).

[41] F. Zhang, C. Hea, L. Cao, W. Feng, H. Wang, X. Moa, J. Wangd, *Int. J. Biol. Macromol.* **48,** 474 (2011).

[42] S. D. Nath, C. Abueva, B. Kima, B. T. Lee, *Carbohydr. Polym.* **115,** 160 (2015).